ELSEVIER

Journal of Alloys and Compounds 408–412 (2006) 1222–1225

Journal of ALLOYS AND COMPOUNDS

www.elsevier.com/locate/jallcom

Thermoelectric power and resistivity in $Nd_{2-x}Ce_xCuO_4$ system

Natsuki Mori [a,*], Takehiro Kameyama [a], Hiroyuki Enomoto [b], Hajime Ozaki [c], Yoshiki Takano [d], Kazuko Sekizawa [d]

[a] *Department of Electrical and Computer Engineering, Oyama National College of Technology, Oyama 323-0806, Japan*
[b] *Department of Materials Science, Osaka Electro-Communication University, Neyagawa 572-8530, Japan*
[c] *Department of Electrical Engineering and Bioscience, Waseda University, Tokyo 169-8555, Japan*
[d] *Department of Physics, Nihon University, Tokyo 101-8308, Japan*

Received 30 July 2004; received in revised form 25 November 2004; accepted 15 December 2004
Available online 17 June 2005

Abstract

The temperature dependence of the resistivity $\rho(T)$ and that of the thermoelectric power $S(T)$ are investigated for electron-doped $Nd_{2-x}Ce_xCuO_4$ system with $0 \leq x \leq 0.1$ prepared by the solid-phase reaction method. As to room-temperature values of these properties upon Ce doping, the system has a maximum in S_{300} at doping level $x \approx 0.01$–0.02 while showing a continuum decrease in ρ_{300}. The behavior of $\rho(T)$ for $30\,K \leq T \leq 300\,K$ obeys an exponential dependence of temperature with its negative slope being reduced as x increases. Variations of $S(T)$ in the range $100\,K \leq T \leq 300\,K$ exhibit a broad peak shifting towards low temperatures as the system approaches to a metallic state. The behavior of $S(T)$ and its doping dependence can be well reconciled with a narrow band model, from which a possible band spectrum is deduced in relevance to hole-doped cuprates.

Keywords: Electronic transport; Thermoelectric power; Resistivity; $Nd_{2-x}Ce_xCuO_4$; Electron doping

1. Introduction

Considerable efforts have been devoted to the researches for developing metal oxides with high performances in thermoelectric properties. One of the most successful results may be the discovery of $NaCo_2O_4$ compounds, the pioneer work of which has been made by Terasaki et al. [1], and consequently many proto-type materials have also been found to give a similar or even better performance [2]. Although there exist many studies of thermoelectric properties in "p-type" oxides, relatively a little attention has been paid to those in "n-type" ones. The compound $Nd_{2-x}Ce_xCuO_4$ (NCCO) of the T′ structure is known to be an electron-doped superconductor at the doping level $x \approx 0.15$ [3]. Despite a growing body of data on the transport properties in NCCO for $x \geq 0.1$ [4-8], little is known about their properties in the highly underdoped regime.

In this article, we report the electrical conduction and thermoelectric effect in NCCO with $0 \leq x \leq 0.1$, envisaging that this system could be an n-type thermoelectric material with a high performance. The thermoelectric power is analyzed in terms of a narrow band model [9,10], from which we could obtain variations of band-spectrum parameters against the Ce content. As far as the present analysis is concerned, we conclude that a main feature of the thermoelectric power in both p-type and n-type cuprates is attributed from the same modifications of the band structure upon carrier doping.

2. Methods of experiment and analysis

Polycrystalline samples under study were prepared by means of a standard solid-phase reaction method. Stoichiometric amounts of oxide powders Nd_2O_3 (99.9%), CeO_2

* Corresponding author. Tel.: +81 285 20 2228; fax: +81 285 20 2880.
E-mail address: mori@oyama-ct.ac.jp (N. Mori).

0925-8388/$ – see front matter © 2005 Elsevier B.V. All rights reserved.
doi:10.1016/j.jallcom.2004.12.147

(99.99%) and CuO (99.99%) were sintered at 1050 °C for totally 48 h in air with an intermediate grinding. The samples were made in a bar shape of 6 mm × 3 mm × 26 mm which was designed to fabricate a Peltier refrigeration device. A reduction procedure, which is usually employed to prepare superconducting samples in order to create more free carriers, was not adopted here. Powder X-ray diffractometry showed all the samples to be a single phase but with small traces of impurity phases for higher Ce contents. Lattice parameters of a and c axes were estimated to be approximately 3.942 and 12.16 Å, respectively, with a tendency that the former increases upon doping while the latter decreases, as reported by others [3,11].

The temperature dependence of the resistivity $\rho(T)$ was measured in the range $30\,\mathrm{K} \le T \le 300\,\mathrm{K}$ by a DC four probe method with a constant current of 0.1–1 mA using a cryostat equipped with a 10 K refrigerator. Measurements on the thermoelectric power $S(T)$ in the temperature range of $100\,\mathrm{K} \le T \le 300\,\mathrm{K}$ were carried out using a liquid nitrogen cryostat, by means of a DC differential method in a similar way as described in Ref. [12] but with copper–constantan thermocouples. For the undoped system, we could not obtain reproducible results for $\rho(T)$ and $S(T)$, probably ascribed to a highly resistive state of the samples.

Data on $S(T)$ in hole-doped cuprates have been analyzed in terms of several theoretical models, other than a simple Fermi-liquid picture which leads to $S(T) \propto T$, including a narrow conduction-band model [9,10], a Boson–Fermion theory [13], a pseudogap model [14] and a two-band theory [15]. Because of the wide availability to both metallic and degenerated semiconducting systems, we will adopt the first model in which spectrum of the conduction-band is assumed to contain a sharp peak near the Fermi level. A comparison to this model can provide insight into the band spectrum through three adjustable parameters: the band-filling factor F, the effective width of the conduction band W_D and that of the delocalized states W_σ. The expression for $S(T)$ takes the form [9,10]:

$$S(T) = -A\frac{k_\mathrm{B}}{e}\left\{\frac{W_\sigma^*}{\sinh W_\sigma^*}\left[\exp(-\mu^*) + \cosh W_\sigma^* - \frac{1}{W_\sigma^*}(\cosh\mu^* + \cosh W_\sigma^*) \times \ln\frac{\exp(\mu^*) + \exp(W_\sigma^*)}{\exp(\mu^*) + \exp(-W_\sigma^*)}\right] - \mu^*\right\} \quad (1)$$

where A is a constant, μ^* is written with the chemical potential μ as:

$$\mu^* = \frac{\mu}{k_\mathrm{B}T} = \ln\frac{\sinh(FW_\mathrm{D}^*)}{\sinh[(1-F)W_\mathrm{D}^*]} \quad (2)$$

and $W_\mathrm{D}^* = \frac{W_\mathrm{D}}{2k_\mathrm{B}T}$, $W_\sigma^* = \frac{W_\sigma}{2k_\mathrm{B}T}$. A physical picture of the model will be given in the next section.

3. Results and discussion

3.1. Room temperature properties

We first present the resistivity ρ_{300} and thermoelectric power S_{300} at room temperature, both of which are plotted in Fig. 1 as a function of Ce content x. The vertical bars indicate ranges of those values in a few samples prepared at each doping level, and the plots represent average values among them. The negative sign of S_{300} was observed for all the samples investigated as expected for a material with electron doping. The system shows a maximum in the S_{300} at $x \approx 0.01$–0.02, though the values at $x = 0.01$ are scattered from sample to sample, and then a rapid reduction with increasing x. On the other hand, the ρ_{300} exhibits a monotonous reduction as x increases, indicating that the addition of Ce provides the carriers.

On the whole, the present results show higher values in both ρ_{300} and S_{300} in comparison to those reported in the literatures [4,8]. This trend indicates that our samples, prepared without taking a reduction stage, may be in a higher oxidation state [16], containing less oxygen deficiency which generates carries in CuO_2 planes. As a measure of characterizing thermoelectric materials, one may evaluate a power factor defined as $P = S^2/\rho$. The power factor P_{300} at room temperature estimated from the average values is displayed in the inset of Fig. 1 as a function of Ce content x, showing its values to be of the same order of magnitude as in other reports [17,18], with all the differences in ρ_{300} and S_{300} themselves.

3.2. Properties of ρ(T)

The behavior of $\rho(T)$ in some of our samples is displayed in Fig. 2, where the resistivity is plotted in a log scale against temperature. At the overall Ce doping levels investigated, samples show semiconducting behavior in the sense that the

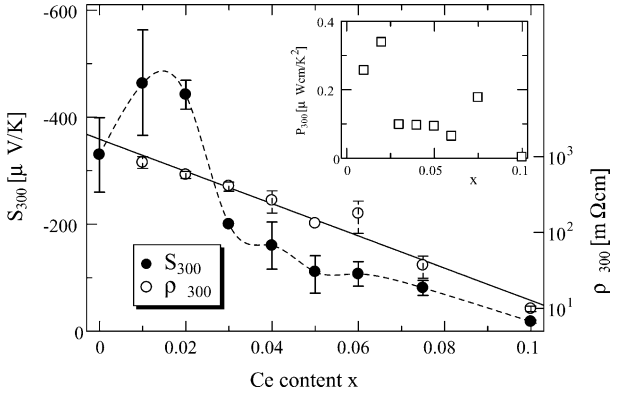

Fig. 1. Room-temperature thermoelectric power S_{300} and resistivity ρ_{300} as a function of Ce content x for the NCCO system. The vertical bars represent ranges of values for different samples. The solid line indicates the least squared fitting line for ρ_{300}, while the broken line is only for the guide to the eye as to S_{300}. The inset shows room-temperature power factor $P_{300} = \frac{S_{300}^2}{\rho_{300}}$ plotted against x.

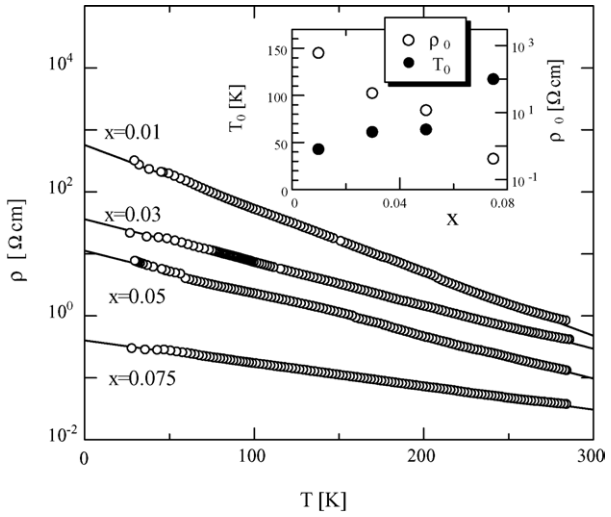

Fig. 2. Behavior of the resistivity $\rho(T)$ in log ρ vs. T plots for some of NCCO samples along with the least squared fits to a relation $\rho(T) = \rho_0 \exp(-T/T_0)$. The inset displays fitting parameters T_0 and ρ_0 plotted against Ce content x.

resistivity increases with decreasing temperature. Although there is only a few available reports on the $\rho(T)$ for the NCCO system with a small Ce content, such a feature is consistent with results obtained for polycrystalline samples [17], while in contrast to those reported for single crystals by Xu et al. [18] in which a metallic conduction has been observed for $100\,\mathrm{K} \leq T \leq 300\,\mathrm{K}$ even in the doping level $x = 0.01$. As evidenced from Fig. 2, ln $\rho(T)$ obeys a linear T-dependence over a whole temperature range measured with a steeper negative slope for lower doping levels. The solid lines represent the least squared fits to a relation $\rho(T) = \rho_0 \exp(-T/T_0)$, and fitting values of T_0 and ρ_0 for each sample are plotted in the inset as a function of x.

A similar type of the conduction may be seen in polycrystalline $Nd_{1.85}Ce_{0.15}CuO_{4-y}$ system obtained by quenching [19] and $Nd_{1.85}Ce_{0.15}Cu_{1+\delta}O_{4-y}$ with excess Cu contents of $0\,\mathrm{K} \leq \delta \leq 0.03\,\mathrm{K}$ [20]. Other recent examples of interest related to the conduction behavior can be found in studies of sample-disordering effects on the $\rho(T)$ for $Nd_{1.85}Ce_{0.15}CuO_{4-y}$ films [21,22], in which a systematic evolution from metallic to semiconducting behavior is shown to appear with developing a degree of disorder. Although theoretical expressions for these results are different from our formula, effects of structural disorder in a microscopic or mesoscopic scale can, it appears, be responsible for observed behavior of the electrical conduction. It is of interest to point out that we have observed a linear ln ρ versus T relation also in p-type $Y_{1-x}Pr_xBa_2Cu_3O_{7-y}$ and Ag-doped $PrBa_2Cu_3O_{7-y}$ bulk systems, in which a fractal or percolative character could be responsible for the transport properties.

3.3. Properties of S(T)

Characteristics of $S(T)$ in samples with $0.01 \leq x \leq 0.075$ are displayed in Fig. 3 together with theoretical fits (the solid lines) to the narrow band model described in the previous section. We point out the following features that would be universal to copper oxide systems: (1) The thermoelectric power significantly depends upon T in the case of a small doping level x (a low carrier density) while that dependence becomes weaker as x increases. (2) $S(T)$ exhibits a broad maximum which shifts towards lower temperature with increasing x. These features have been reported for a variety of hole-doped cuprate systems [9,10,13–15,23].

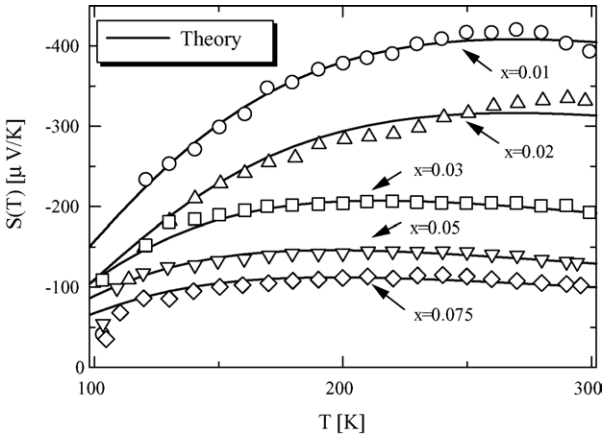

Fig. 3. Behavior of the thermoelectric power $S(T)$ of the NCCO system together with theoretical fits (the solid lines) to Eqs. (1) and (2) based on the narrow band model.

Theoretical fits to Eqs. (1) and (2) allow us to determine the band spectrum parameters F, W_D and W_σ. In order to reproduce the present results, we have to introduce a factor $A = 9.0$ fixed to be constant throughout the analysis. Fitting values of other parameters are plotted in the main part (the filling factor F) and the inset (the band widths W_D and W_σ) of Fig. 4 against the Ce content, showing systematic variations upon doping. Increasing F towards to the half filled state ($F = 0.5$) is consistent with donating electrons from Ce ions. Starting

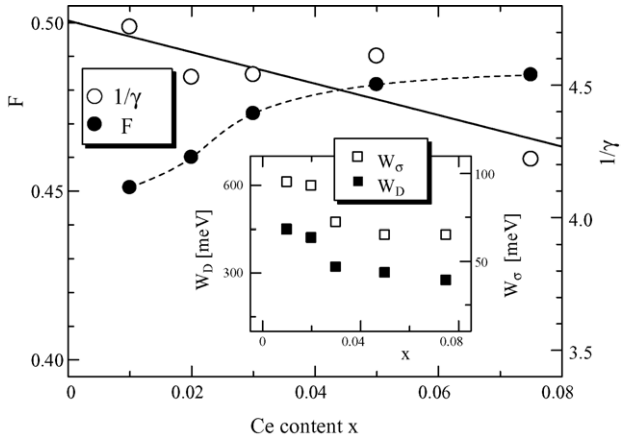

Fig. 4. The main part displays values of the electron filling F and a degree of the electron localization $1/\gamma \equiv (W_\sigma/W_D)^{-1}$ as a function of Ce content x, obtained from the theoretical fits in Fig. 3. The lines along with plots are only for the guide to the eye. The inset exhibits the width of the conduction band W_D and that of the delocalized states W_σ upon doping.

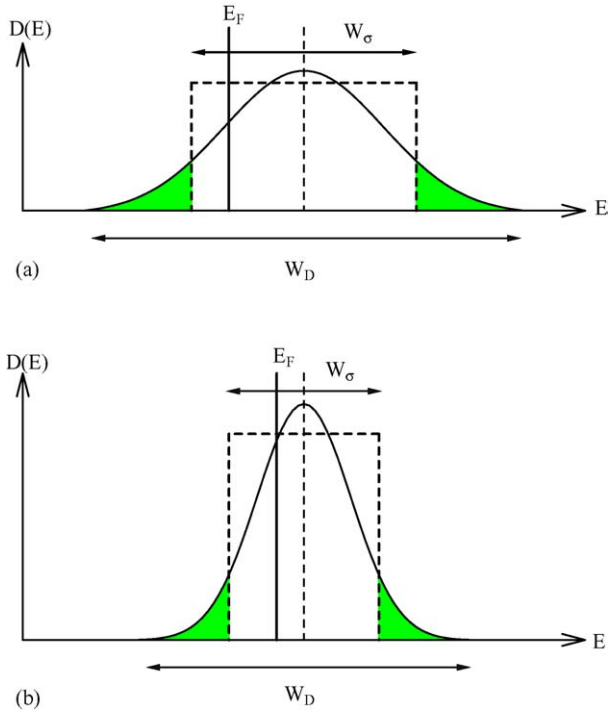

Fig. 5. Schematic illustrations of the density of states $D(E)$ in the conduction band deduced from the analysis of $S(T)$ shown in Figs. 3 and 4, for the cases of (a) a low Ce content and (b) a high Ce content. The shaded parts denote localized electron states, and the position of the Fermi level E_F is indicated by the thick vertical line.

from the insulator side ($x = 0$), while both bandwidths become narrower, the ratio $1/\gamma \equiv (W_\sigma/W_D)^{-1}$ regarded as the degree of the electron localization tends to reduce on approaching to the metallic region. The behavior is represented by the solid line (the least squared fit) in Fig. 4. Although $S(T)$ properties described by Eq. (1) depend complicatedly upon the parameters, roughly speaking it is anticipated that the magnitude of the thermoelectric power is sensitive to a change in F while the ratio $1/\gamma$ determines the way in which $S(T)$ varies. A picture of the density of states $D(E)$ deduced from the above analysis is schematically illustrated in Fig. 5 for the cases of (a) a low doping level and (b) a high doping level. This figure shows that, with increasing Ce dopant, the Fermi level E_F (denoted by the thick vertical line) shifts towards higher energy and that localized electron states (the shaded parts) become narrower.

4. Conclusion

We have investigated thermoelectric power S and electrical resistivity ρ in $Nd_{2-x}Ce_xCuO_4$ bulk system with $0 \leq x \leq 0.01$. The room temperature value of S in the system shows a maximum at $x \approx 0.01$–0.02, leading to a maximal power factor $P \approx 0.4\,\mu W\,cm/K^2$, which is unfortunately much lower than values for practical purposes. We have observed behavior of $\rho(T)$ giving a linear $\ln \rho(T)$ versus T relation, for which no plausible explanation has been made as yet though we have occasionally encountered such evidence in literatures. Overall features observed in the $S(T)$ upon carrier doping could be attributed not only to the change in the carrier density but also to the modification of the band spectrum, due perhaps to the hybridization of states, in much the same way as in hole-doped cuprates.

Acknowledgments

The authors would like to thank H. Okano, S. Nakakuki, S. Azegami and T. Araki for their assistance in sample preparation and measurements. This study was partly supported by Grant-in-Aid for Scientific Research No. 16560019 (2004) from the Ministry of Education, Culture, Sports, Science and Technology in Japan.

References

[1] I. Terasaki, Y. Sasago, K. Uchinokura, Phys. Rev. B 56 (1997) R12685.
[2] See, for example, Proceedings of 17th International Conference on Thermoelectronics (ICT98), The Institute of Electrical and Electronics Engineers, Inc., Tokyo, 1998.
[3] H. Takagi, S. Uchida, Y. Tokura, Phys. Rev. Lett. 62 (1989) 1197.
[4] J. Takeda, T. Nishikawa, M. Sato, Physica C 231 (1994) 293.
[5] E.J. Singley, D.N. Basov, K. Kurahashi, T. Uefuji, K. Yamada, Phys. Rev. B 64 (2001) 224503.
[6] V. Pankov, N. Kalanda, V. Truchan, D. Zhigunov, O. Babushkin, Physica C 377 (2002) 521.
[7] T.R.E. Hammad, R. Horyn, E. Bukowska, A.J. Zaleski, Physica C 387 (2003) 208.
[8] H.S. Yang, Y.S. Chai, J. Liu, M. Yu, P.C. Li, L. Zhang, M.D. Li, L.Z. Cao, Physica C 403 (2004) 203.
[9] V.E. Gasumyants, V.I. Kaidanov, E.V. Vladimirskaya, Physica C 248 (1995) 255.
[10] V.E. Gasumyants, E.V. Vladimirskaya, I.B. Patrina, Phys. Solid State 39 (1997) 1352.
[11] J.L. Peng, Z.Y. Li, R.L. Greene, Physica C 177 (1991) 79.
[12] V.V. Rao, G. Rangarajan, R. Srinivasan, J. Phys. F 14 (1984) 973.
[13] X.H. Chen, T.F. Li, M. Yu, K.Q. Ruan, C.Y. Wang, L.Z. Cao, Physica C 290 (1997) 317.
[14] Q.M. Zhang, X.S. Xu, X.N. Ying, A. Li, Q. Qiu, Y.N. Wang, G.J. Xu, Y.H. Zhang, Physica C 337 (2000) 277.
[15] S.R. Ghorbani, P. Lundqvist, M. Andersson, M. Valldor, O. Rapp, Physica C 353 (2001) 77.
[16] P.A. van Aken, W.F. Muller, J. Choisnet, Physica C 211 (1993) 421.
[17] M.-Y. Choi, J.S. Kim, Phys. Rev. B 59 (1999) 192.
[18] X.-Q. Xu, S.J. Hagen, W. Jiang, J.L. Peng, Z.Y. Li, R.L. Greene, Phys. Rev. B 45 (1992) 7356.
[19] A. Seffar, J. Fontcuberta, S. Pinol, J.L. Garcia-Munoz, X. Obradors, G. Peraudeau, R. Berjoan, Physica C 235–240 (1994) 791.
[20] F. Prado, J. Briatico, A. Serquis, A. Caneiro, M. Tovar, M.T. Causa, Physica C 235–240 (1994) 785.
[21] G.I. Harus, A.I. Ponomarev, T.B. Charikova, A.N. Ignatenkov, L.D. Sabirzjanova, N.G. Shelushinina, V.F. Elesin, A.A. Ivanov, I.A. Rudnev, Physica C 383 (2002) 207.
[22] S.I. Woods, A.S. Katz, S.I. Applebaum, M.C. de Andrade, M.B. Maple, R.C. Dynes, Phys. Rev. B 66 (2002) 014538.
[23] V.E. Gasumyants, M.V. Elizarova, R. Suryanarayanan, Phys. Rev. B 61 (2000) 12404 (References cited therein).